Inorg. Chem. **2007**, *46*, 11031–11035

Temperature-Triggered Self-Assembly of ZnO: from Nanocrystals to Nanorods to Tablets

Yong Hu,*,† Ting Mei,*,† Jun Guo,‡ and Tim White‡

School of Electrical and Electronic Engineering and School of Materials Science and Engineering, Nanyang Technological University, Singapore 639798, Singapore

Received May 4, 2007

ZnO nanocrystals, nanorods, and tablets were prepared at 110, 140, and 180 °C in a water–ethanol system. Nanorods (~2 × 40 nm) arranged in serpentine morphologies formed by the oriented coalescence of anhedral ZnO nanocrystals (~3.5 nm diameter), while tabular ZnO grew by [$\bar{1}2\bar{1}0$] textural attachment of the nanorods. The development of these crystal habits is believed to proceed via a dissolution and growth mechanism mediated by a transient amorphous phase. Materials synthesized at intermediate temperatures (125 and 160 °C) possessed microstructures containing mixed crystal forms in the expected orientation relationship. Photoluminescent spectra of the nanocrystals and nanorods showed blue shifts of 0.16 and 0.13 eV with respect to the bulk ZnO band gap (3.26 eV) due to quantum confinement, with the narrow emission peaks typical of particles possessing uniform size and shape. The larger tablets displayed a less energetic emission (3.10 eV) ascribed to exciton–exciton collisions.

Introduction

In recent years, nanostructured semiconductors have been extensively investigated for nanoelectronic and optoelectronic applications due to their special electrical and optical properties. Zinc oxide is an important functional II−VI compound semiconductor due to its wide direct band gap ($E_g = 3.3$ eV), large exciton binding energy ($E_B = 60$ meV), and other attractive properties, including its piezoelectric characteristics, chemical stability, and biocompatibility. It has been widely adopted in applications such as optoelectronic switches, high-efficiency photonic devices, ultraviolet (UV) lasers, sensors, and three-dimensional nanoscale self-assembly systems.[1−3] ZnO nanostructures are diverse, crystallographically well-defined, and include nanoneedles, nanocables and nanotubes, nanowalls, nanobridges and nanonails, nanohelixes, nanosprings, nanorings, hierarchical nanostructures, and mesoporous polyhedral cages and shells.[4−11] By selecting the appropriate ZnO architecture, less favorable characteristics such as weak exciton emission compared with defect-related (deep-level) visible emission can be eliminated, while retaining or enhancing desirable properties such as large exciton binding energies, that in combination with strong exciton emission allow for stable high-yield luminescence at room temperature.

A number of methods have proven successful for the reproducible growth of ZnO crystals of specific size and shape, such as thermal evaporation, vapor-phase transport, laser ablation, gamma-ray irradiation, metal−organic chemical vapor deposition, hydrothermal growth, and template-assisted solution processes.[12−22] Among these, the hydrothermal treatment of reactants in aqueous solutions is a

* To whom correspondence should be addressed. E-mail: huyong@ntu.edu.sg (H.Y.), ETMei@ntu.edu.sg (T.M). Tel: 0065-67904387. Fax: 0065-67904161.

† School of Electrical and Electronic Engineering.

‡ School of Materials Science and Engineering.

(1) Xia, Y. N.; Yang, P. D.; Sun, Y.; Wu, Y.; Mayers, B.; Yin, Y.; Kim, F.; Yan, H.; *Adv. Mater.* **2003**, *15*, 353.
(2) Pan, Z. W.; Dai, Z. R.; Wang, Z. L. *Science* **2001**, *291*, 1947.
(3) Hu, J.; Odom, T. W.; Lieber, C. M. *Acc. Chem. Res.* **1999**, *32*, 435.
(4) Park, W. I.; Yi, G. C.; Kim, M.; Pennycook, S. J. *Adv. Mater.* **2002**, *14*, 1841.
(5) Hu, J. Q.; Li, Q.; Meng, X. M.; Lee, C. S.; Lee, S. T. *Chem. Mater.* **2003**, *15*, 305.
(6) Lao, J. Y.; Huang, J. Y.; Wang, D. Z.; Ren, Z. F.; Steeves, D.; Kimball, B.; Porter, W. *Appl. Phys. A: Mater. Sci. Process.* **2004**, *78*, 539.
(7) Lao, J. Y.; Huang, J. Y.; Wang, D. Z.; Ren, Z. F. *Nano Lett.* **2003**, *3*, 235.
(8) Kong, X. Y.; Wang, Z. L. *Nano Lett.* **2003**, *3*, 1625.
(9) Kong, X. Y.; Ding, Y.; Yang, R.; Wang, Z. L. *Science* **2004**, *303*, 1348.
(10) Lao, J. Y.; Wen, J. G.; Ren, Z. F. *Nano Lett.* **2002**, *2*, 1287.
(11) Gao, P. X.; Wang, Z. L. *J. Am. Chem. Soc.* **2003**, *125*, 1299.
(12) Huang, M.; Mao, S.; Feick, H.; Yan, H.; Wu, Y.; Kind, H.; Weber, E.; Russo, R.; Yang, P. D. *Science* **2001**, *292*, 1897.
(13) Huang, M.; Wu, Y.; Feick, H.; Tran, N.; Weber, E.; Yang, P. D. *Adv. Mater.* **2001**, *13*, 113.
(14) Wu, J. J.; Liu, S. C. *Adv. Mater.* **2002**, *14*, 215.

10.1021/ic700863g CCC: $37.00
Published on Web 11/28/2007

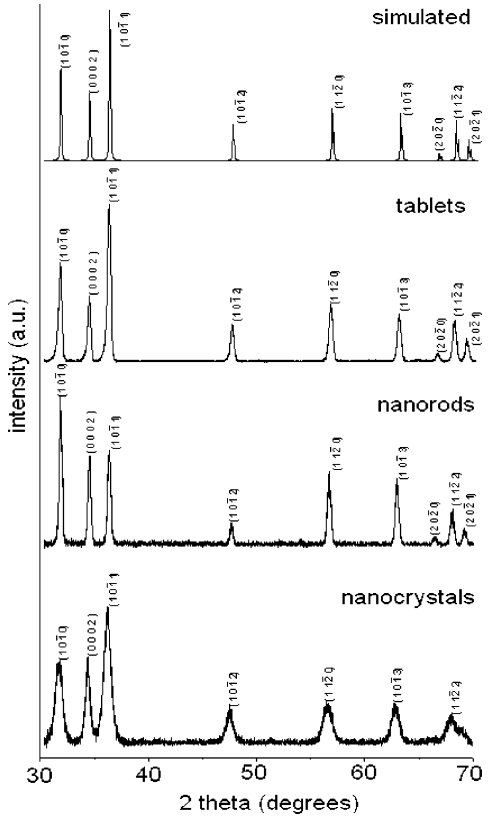

Figure 1. XRD patterns of ZnO nanocrystals, nanorods, tablets, and simulation.

relatively simple and effective way to fabricate ZnO nanostructures under low supersaturation and mild conditions.

Recently, ZnO nancrystals with various shapes have been synthesized using different surfactants, such as trioctylphosohine oxide, oleic acid, 1-hexadexylamine, *tert*-butylphosphonic acid, and tetradecylphosphonic acid.[23−26] A significant advance in the general synthesis of nanocrystals, including noble-metal, semiconductor, and rare-earth fluorescing nanocrystals is the liquid−solid−solution (LSS) strategy based on the phase transfer and separation processes across the interfaces.[27−29] By tailoring interfacial chemical reactions, an extensive group of nanocrystals of tunable sizes and with hydrophobic surfaces was prepared.

This paper describes a modification the LSS approach for the synthesis of ZnO nanocrystals in which the base sodium linoleate was replaced by NaOH, whose higher water solubility makes precipitation stable and controllable. Although self-assembly of micron-sized aggregates is a well-known phenomenon in colloid chemistry,[30] kinetic models describing this type of growth do not consider the process on an atomic level nor attend to the crystallographic orientation of the aggregated particles. Therefore, these features require experimental investigation. In this present study, temperature-triggered self-assembly growth mechanisms[31] yield nearly perfectly monodisperse ZnO nanocrystals, serpentine nanorods, and tablets as a function of temperature. It was found that oriented attachment of the preformed anhedral ZnO nanoparticles leads to high-quality crystalline nanorods, and further assembly of these yields yields textured nanotablets. This growth sequence was examined by high-resolution transmission electron microscopy (HRTEM) and powder X-ray diffraction (XRD). The photoluminescence (PL) of the nanocrystals and nanorods exhibit obvious blue-shifted emission, indicating uniform size.

Experimental Section

Synthesis of ZnO Nanocrystals, Nanorods, and Tablets. All the chemical reagents were purchased from Sigma-Aldrich and used without further purification. Deionized water was used throughout. The ZnO nanocrystals were synthesized as follows. A homogeneous solution was prepared from 4 mL (12.87 mmol) of linoleic acid, 0.5 g of NaOH, and 16 mL of ethanol by stirring at room temperature. Subsequently, 0.5 g of $ZnCl_2$ was dissolved in 7 mL of deionized water by ultrasonic vibration for 5 min. The mixed solution was obtained by adding these together and maintained at room temperature for a few minutes under stirring. Finally, the mixed reactants were transferred to a Teflon-lined, 40 mL stainless-steel autoclave that was sealed and heated at 110 °C for 10 h. The system was allowed to cool to room temperature, and the product was collected by centrifugation. The product was washed three times with deionized water and absolute ethanol. The preparation of nanorods and tablets was identical except that the hydrothermal reactions were conducted at 140 and 180 °C, respectively. ZnO was also produced at the intermediate temperatures of 125 and 160 °C.

Characterization. Powder XRD measurement of the sample was performed with a Siemens D5005 X-ray diffractometer using Cu Kα radiation at a scanning rate of 0.06° s^{-1}. Field emission scanning electron microscopy (FE-SEM) was performed with a JEOL JSM-6700 field-emission scanning electron microanalyzer with an accelerating voltage of 15 keV. Transmission electron microscopy (TEM) was conducted at 200 keV with a JEM-2100F field emission machine. Samples were prepared for TEM by dispersing the hydrothermal products in ethanol and placing several drops of the suspension on holey carbon films supported by copper grids. Both FE-SEM and TEM observations were made without the need to deposit a conductive coating. The PL spectra were measured at

(15) Zheng, M. J.; Zhang, L. D.; Li, G. H.; Shen, W. Z. *Chem. Phys. Lett.* **2002**, *363*, 123.
(16) Liu, C. H.; Zapien, J. A.; Yao, Y.; Meng, X. M.; Lee, C. S.; Fan, S. S.; Lifshitz, Y.; Lee, S. T. *Adv. Mater.* **2003**, *15*, 838.
(17) Gao, P. X.; Ding, Y.; Wang, Z. L. *Nano Lett.* **2003**, *3*, 1315.
(18) Yao, D. B.; Chan, Y. F.; Wang, N. *Appl. Phys. Lett.* **2002**, *81*, 757.
(19) Hu, Y.; Chen, J. F.; Xue, X.; Li, T. W.; Xie, Y. *Inorg. Chem.* **2005**, *44*, 7280.
(20) Vayssieres, L. *Adv. Mater.* **2003**, *15*, 464.
(21) Greene, L. E.; Law, M.; Goldberger, J.; Kim, F.; Johnson, J. C.; Zhang, Y.; Saykally, R. J.; Yang, P. D. *Angew. Chem.* **2003**, *42*, 3031.
(22) Liu, B.; Zeng, H. C. *J. Am. Chem. Soc.* **2003**, *125*, 4430.
(23) Joo, J.; Kwon, S. G.; Yu, J. H.; Hyeon, T. *Adv. Mater.* **2005**, *17*, 1873.
(24) Andelman, T.; Gong, Y. Y.; Polking, M.; Yin, M.; Kuskovsky, I.; Neumark, G.; O'Brien, S. *J. Phys. Chem. B* **2005**, *109*, 14314.
(25) Cozzoli, P. D.; Curri, M. L.; Agostiano, A.; Leo, G.; Lomascolo, M. *J. Phys. Chem. B* **2003**, *107*, 4756.
(26) Chen, Y. F.; Kim, M.; Lian, G. D.; Johnson, M. B.; Peng, X. G. *J. Am. Chem. Soc.* **2005**, *127*, 13331.
(27) Wang, X.; Zhuang, J.; Peng, Q.; Li, Y. D. *Nature* **2005**, *437*, 121.
(28) Wang, X.; Zhuang, J.; Peng, Q.; Li, Y. D. *Adv. Mater.* **2006**, *18*, 2031.
(29) Liang, X.; Wang, X.; Zhuang, J.; Chen, Y. T.; Wang, D. S.; Li, Y. D. *Adv. Funct. Mater.* **2006**, *16*, 1813.
(30) Park, J.; Privman, V.; Matijevic, E. *J. Phys. Chem. B* **2001**, *105*, 11630.
(31) Pacholski, C.; Kornowski, A.; Weller, H. *Angew. Chem., Int. Ed.* **2002**, *41*, 1188.

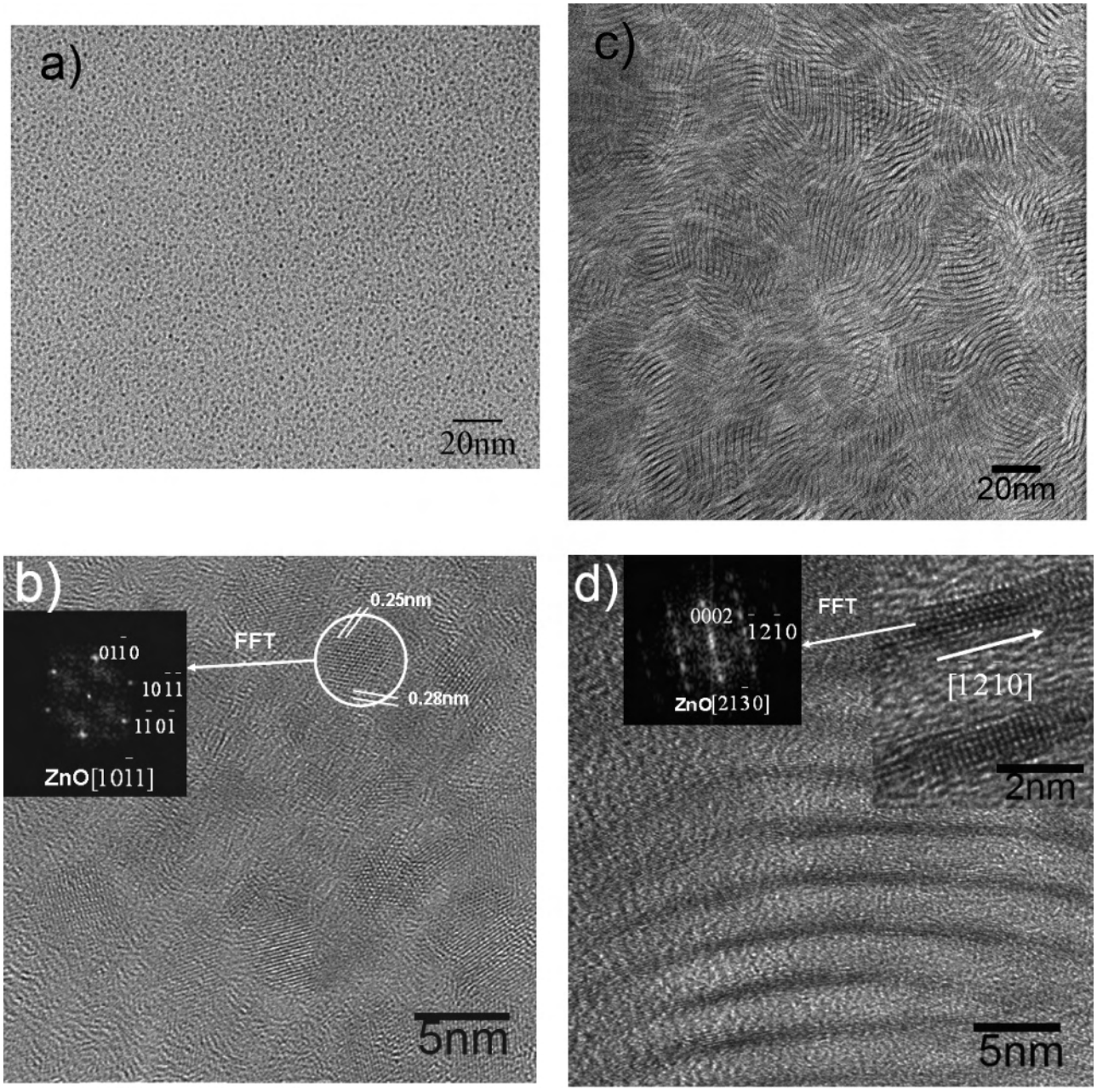

Figure 2. (a) TEM image of ZnO nanocrystals at 110 °C. (b) HRTEM image with FFT of ZnO nanocrystals. (c) TEM image of local ordered ZnO nanorods at 140 °C. (d) HRTEM image with FFT of ZnO nanorods and higher magnification image (inset).

room temperature with a Fluorolog-3 spectrofluorimeter using an excitation wavelength of 325 nm.

Results and Discussion

All reflections in the XRD patterns are shown in Figure 1, which was indexed as wurtzite-structured ZnO (JCPDS card no. 89-0511) with nominal cell constants of $a = 3.249$ Å and $c = 5.205$ Å, and impurities such as $Zn(OH)_2$ were not detected. The ZnO nanocrystals (110 °C product) and nanorods (140 °C) show texture with size-broadened reflections, while the tablets (180 °C) are larger with narrow reflections and no obvious preferred orientation. For the crystals synthesized at 110 °C, Scherrer analysis of all the Bragg reflections yielded an average crystal diameter of ~3.5 nm which was consistent with the bright field TEM images shown in Figure 2a. By comparing simulated XRD patterns with observed diffraction intensities, it is evident that the low-dimensional structures (crystals and rods) possess distinct texture while the larger tablets do not display preferred orientation.

Figure 2b shows the HRTEM image with fast-Fourier transform (FFT) of the ZnO nanocrystals, at the unit cell scale, where alignment was along a principal axis. Fourier reconstruction yielded patterns consistent with wurzite. The TEM image (Figure 2c) of the sample synthesized at 140 °C shows that the products were composed of many local ordered serpentine nanorods of about 2 nm in width and 40 nm in length. Seen from the HRTEM image with FFT (Figure 2d) and the higher magnification image (inset), the

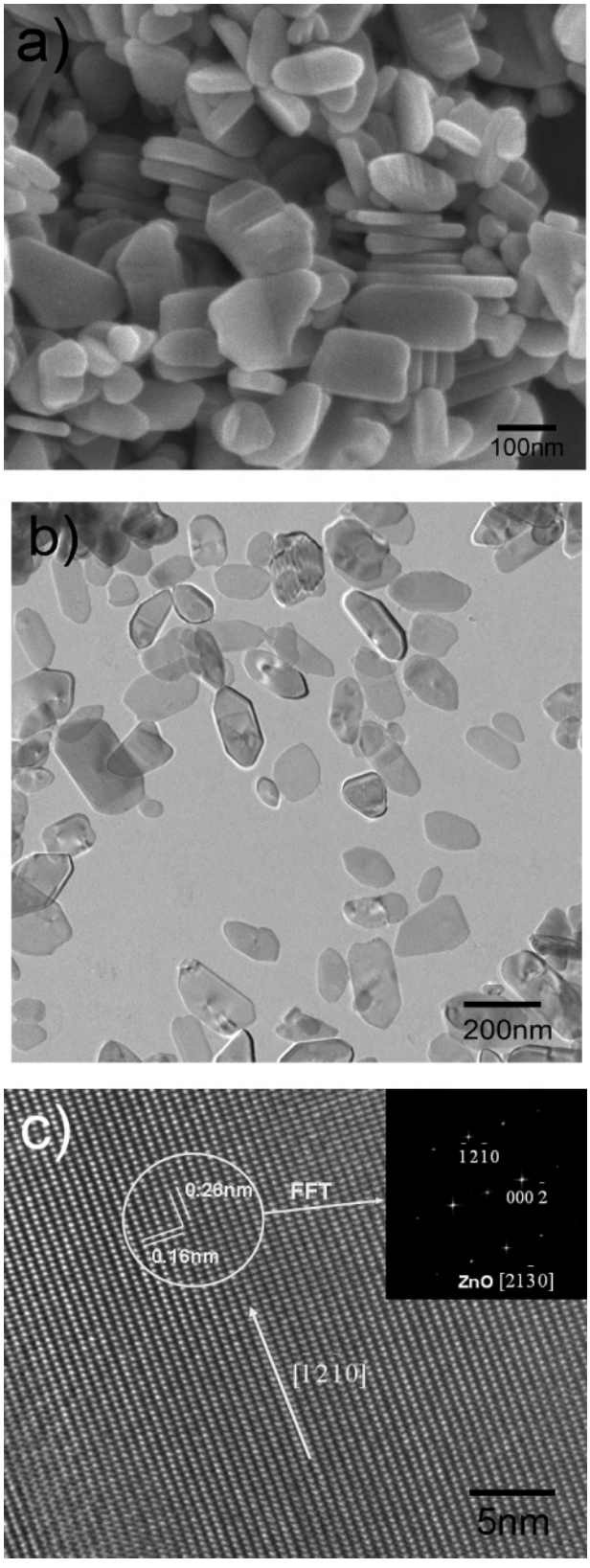

Figure 3. (a) FE-SEM image of ZnO nanotablets at 180 °C. (b) TEM image of ZnO nanotablets. (c) HRTEM image with FFT of ZnO nanotablets.

nanorods were formed by the accumulation of nanocrystals in the growth direction [$\bar{1}2\bar{1}0$].

The FE-SEM image of the products synthesized at 180 °C shown in Figure 3a reveals larger monodispersed tabular

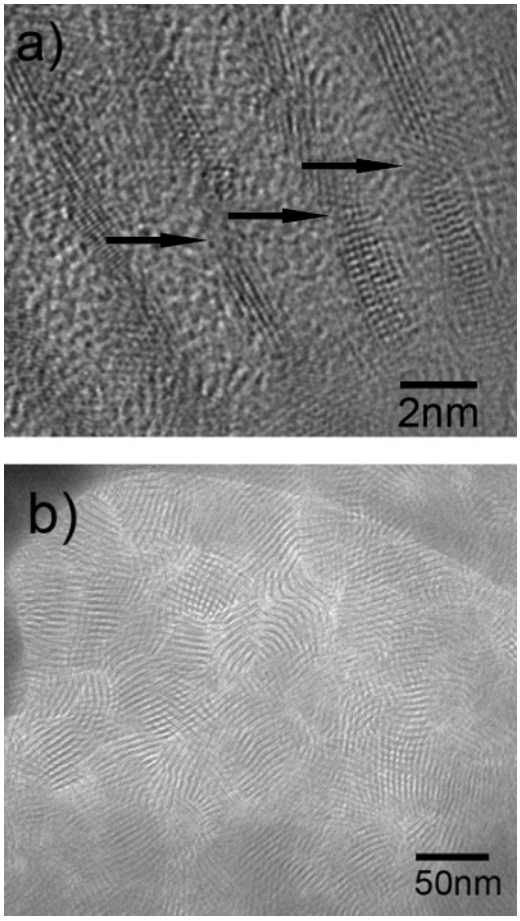

Figure 4. (a) HRTEM image of the oriented attachment ZnO nanocrystals at 125 °C. (b) TEM image of the local ordered aggregated ZnO nanorods at 160 °C.

tablets ~200−300 nm in length and ~50−100 nm in width. Parts b and c of Figure 3 show the TEM and HRTEM (with FFT) images of tablets that are formed by the oriented coalescence of nanorods with preferential development of ($\bar{1}2\bar{1}0$) facets at higher temperature.

At the lowest reaction temperature, crystals were formed, whereas medium reaction temperatures brought forward rods. The highest reaction temperature finally led to the formation of tablets, while intermediate conditions only showed partially developed morphologies. As shown in Figure 4a, at an intermediate condition (125 °C for 10 h) the nascent "nanorods" were composed of several nanocrystals attached by apparently aperiodic and poorly ordered materials (arrowed in Figure 4a). Figure 4b shows the oriented attachment of nanorods at 160 °C for 10 h, where tablet formation is incomplete compared with the 180 °C products. The ZnO morphologies obtained under various conditions are summarized in Table 1.

Both the textures observed by XRD and direct observations of morphology are consistent with the oriented attachment of anhedral ZnO crystals seeding the formation of nanorods that at higher temperature coalesce as tablets. It is suggested that this occurs by the dissolution and growth of particles, as the crystalline portions are separated by decreasing quantities of amorphous and poorly ordered materials (Figure 4a) via an Ostwald ripening process that yields serpentine

Table 1. Relationship between Morphology and Reaction Temperatures

no.	reaction temperature (°C)	growth time (h)	morphology of ZnO
1	110	10	anhedral nanocrystals
2	125	10	aggregated nanocrystals + nanorods
3	140	10	serpentine nanorods
4	160	10	ordered nanorod aggregates
5	180	10	tablets

Scheme 1. Schematic Illustration of Crystal Growth as a Function of Hydrothermal Reaction Temperature: (a) Small Anhedral Crystals of Indistinct Habit Form at 110 °C. (b) Nanocrystals Coalesce to Form Nanorods at 140 °C. (c) Nanorods Condense as Large Tablets with Well-Developed (0002) Surfaces at Higher Temperature

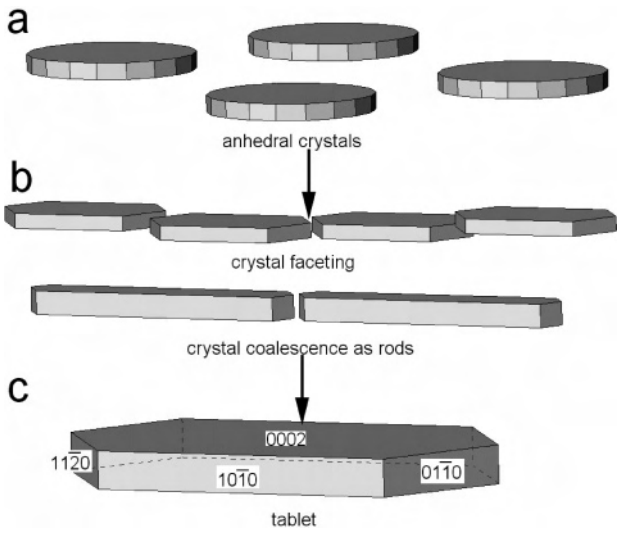

structures and tabular tablets. Elsewhere, it has been reported that self-assembly is driven by increasing particle concentration under solvent evaporation and refluxing colloidal solutions.[31] In this case, temperature plays a similar defining role during hydrothermal synthesis. To further illustrate the growth mechanism, the changes in crystal faceting that occur as a function of hydrothermal reaction temperature are depicted in Scheme 1. At 110 °C small anhedral crystals of indistinct habit are presented (Scheme 1a), while at 140 °C these crystals coalesce to form nanorods of distinct habit that are elongated along $[\bar{1}2\bar{1}0]$ (Scheme 1b), which condense as large tablets with well-developed (0002) surfaces (Scheme 1c). These morphologies develop via a dissolution and growth mechanism.

The PL spectra of the nanocrystals, nanorods, and tablets were measured at room temperature with the excitation at a wavelength of 325 nm, as shown in Figure 5. For the nanocrystals and nanorods, strong excitonic emission peaks are clearly observed at wavelengths of 362 and 366 nm, which correspond to transition energies of 3.42 and 3.39 eV respectively. As a result of quantum confinement induced by the small dimensions, the peaks are blue-shifted by 0.16 and 0.13 eV with respect to the edge emission gap energy (3.26 eV) of bulk ZnO crystals.[32] The narrow width and clear observation of the shifted peaks denotes good size and shape

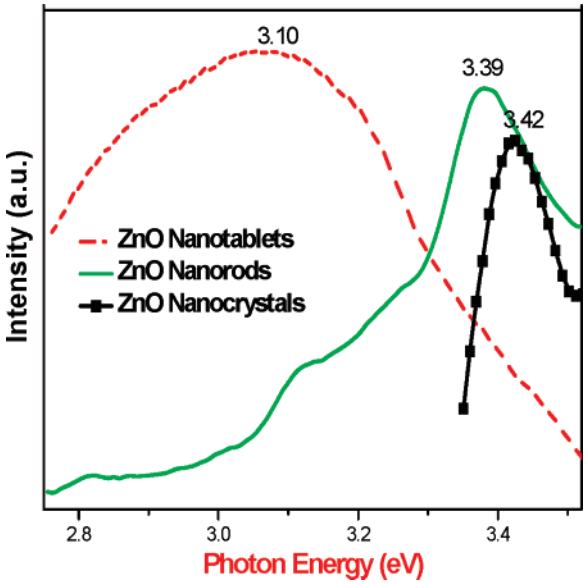

Figure 5. PL spectra of ZnO nanocrystals, nanorods, and nanotablets (λ_{ex} = 325 nm).

uniformity of the products. For tablets, a broad PL spectrum peaking at a wavelength of 400 nm or transition energy of 3.10 eV was observed. The PL at this peak is believed to originate from exciton−exciton collisions,[33] but in general, exciton emission and its phonon replica also contribute to the broadening of PL emission at room temperature.

Conclusion

Monodispersed ZnO nanocrystals were synthesized using a LSS process from water−ethanol solutions. Temperature-dependent oriented coalescence of anhedral nanocrystals initiates the development of serpentine nanorods and tablets, with the growth of these morphologies controlled by a dissolution−precipitation mechanism in which crystallization may be mediated by a transient amorphous phase. The blue shifts seen in the PL spectra of both nanocrystals and nanorods are signatures of structures with low dimensionality (dots and rods). The presented growth mechanism offers an excellent tool to design advanced materials with anisotropic material properties. This would allow the possibility of the synthesis of more complex crystalline three-dimensional structures in which the branching sites could be added as individual nanoparticles. It also may stimulate technological interest and foster many applications in material fields.

Acknowledgment. The authors gratefully acknowledge the financial support (Research Grant No. ARC 2/05) from the Ministry of Education (MOE) and the Agency for Science, Technology and Research (A*STAR), Singapore.

IC700863G

(32) Wang, L. J.; Giles, N. C. *J. Appl. Phys.* **2003**, *94*, 973.
(33) Chen, J. G.; Guo, C. X.; Zhang, L. L.; Hu, J. T. *Chin. Phys. Lett.* **2004**, *7*, 1366.